Biochimica et Biophysica Acta, 946 (1988) 135–142
Elsevier

BBA 74247

Blocking kinetics of Cl^- channels in colonic carcinoma cells (HT_{29}) as revealed by 5-nitro-2-(3-phenylpropylamino)benzoic acid (NPPB)

Jörg Dreinhöfer, Heinz Gögelein and Rainer Greger *

Max-Planck-Institut für Biophysik, Frankfurt / Main (F.R.G.)

(Received 4 July 1988)

Key words: Kinetics; Chloride channel; Channel blocker; (HT_{29} carcinoma cells)

The blocking effect of 5-nitro-2-(3-phenylpropylamino)benzoic acid (NPPB) was investigated on single Cl^- channels of the cultured human colon carcinoma cells, HT_{29}. In the absence of NPPB, the open-time histogram yielded two time constants, with 0.9 ms and 33 ms, whereas the closed-time distribution could be fitted by a single exponential with a time constant of 0.7 ms. Addition of NPPB in the range 1–50 μM induced brief closing events of the single-channel current. This resulted in a decrease of the long open-time constant to 2.1 ms and in an increase of the closed-time constant to 1.8 ms at 50 μM NPPB concentration. The short open-time constant did not change at low blocker concentration (1 μM), but could no longer be resolved at higher concentrations. The open-state probability decreased from 0.9 (control conditions) to 0.5 at 50 μM NPPB. The Hill plot yielded a Hill coefficient of about 0.7, compatible with one NPPB molecule inhibiting one channel molecule. The kinetics of channel gating are described by a sequential model with one closed and two open states. Since in the presence of NPPB no additional time constant appeared in the time histograms, we assumed the same kinetic scheme as under control conditions, and hypothesize that NPPB has an influence on rate constants.

Introduction

It was previously demonstrated that DPC and related substances are potent blockers of the Cl^- conductance in the basolateral membrane of the thick ascending limb of Henle's loop of the rabbit kidney (Refs. 1, 2; reviewed in Ref. 3). NPPB inhibited the Cl^- conductance in this preparation half-maximally at a concentration of $8 \cdot 10^{-8}$ M [2]. The blocking effect of DPC or NPPB on Cl^- channels was observed in a number of other epithelia (reviewed in Ref. 4), as, for example, in the rectal gland of the dogfish [5], pancreatic duct [6], and in the cultured human colon carcinoma cell line HT_{29} [7]. Patch-clamp experiments demonstrated directly that NPPB inhibits single Cl^- channels in the rectal gland of the dogfish [5] and in HT_{29} cells [7]. It was observed that the substance acted by inducing fast closing events (flickering). In order to characterize further the interaction of NPPB with epithelial Cl^- channels, we investigated open- and closed-time distributions of single channels in HT_{29} cells at different blocker concentrations.

Part of this work was published previously in abstract form [8].

* Present address: Physiologisches Institut, Albert-Ludwigs-Universität, Freiburg, F.R.G.

Abbreviations; NPPB, 5-nitro-2-(3-phenylpropylamino)benzoic acid; DPC, diphenylamine-2-carboxylate; cTALH, thick ascending limb of Henle's loop.

Correspondence: H. Gögelein, Max-Planck-Institut für Biophysik, Kennedyallee 70, D-6000 Frankfurt/Main 70, F.R.G.

Materials and Methods

Cell culture

As described previously [7], HT_{29} cells were grown as monolayers in Dulbecco modified Eagle's medium with 15 mM Na-Hepes buffer (pH 7.5), 40 mg penicillin and 90 mg streptomycin per litre, 4 mM L-glutamine, and 100 g/l newborn calf serum in 5% CO_2. Confluent monolayers were subcultured with 0.45 mM EDTA in Ca^{2+}- and Mg^{2+}-free phosphate-buffered saline at intervals of 5–7 days. In these experiments cells were grown on glass cover slips from passages 63 to 90, and were used for patch-clamp studies 3–7 days after subculture.

Experimental details

Cells grown near confluence were studied on the stage of an inverted microscope (Zeiss, IM35) at room temperature. Data recording and analysis were similar to those described in previous reports [9–11]. Patch pipettes were manufactured from borosilicate glass (o.d. 1.5 mm, i.d. 0.9 mm), and were fire-polished. When filled with physiological saline, the resistance of the pipettes was 5–10 MΩ. The preamplifier of the patch-clamp amplifier (L/M EPC7, List, Darmstadt, F.R.G.) was mounted on a micromanipulator, consisting of piezo elements (patch-clamp tower, List). This type of micromanipulator enables precise movements over a distance of 100 μm in all three dimensions. The piezo elements were mounted on micrometer plates, which allow coarse movements in the x, y and z directions. These plates were equipped with remote-controlled electrical motors (own workshop, W. Hampel). This arrangement enables fast positioning of the patch pipette close to the cells. Data were stored on VHS video tapes with a conventional video recorder (Blaupunkt RTV 315, Hildesheim, F.R.G.) after they had been digitized with a pulse-code modulator (PCM 501, Sony, Köln, F.R.G.). As described elsewhere [12], the bandwidth of this instrument was extended to direct current by removing coupling capacitors. Moreover, the filters LPF 102 and LPF 202 were replaced by filters with Bessel characteristics (4-pole, bandwidth 9 kHz). In order to avoid temperature-dependent drifts of the DC signals, a fan was mounted onto the top cover of the instrument. The DC drift was less than ±5 mV after this modification.

The analogue signals were analyzed off-line with a LSI 11/23 computer system. After low-pass filtering (4-pole Bessel, −3 dB 1–2 kHz), the data were sampled with 5–10 kHz and were stored on hard disk. The signals were displayed blockwise on a digital display (HP 1345A, Hewlett Packard), where levels for the baseline (closed channels) and the open state were set under optical control. With the half-maximum threshold method [10] an idealized current trace was constructed and the distribution of the open and closed times as well as the open-state probability, P_o, were calculated. For displaying the open- and closed-time histograms, the data were grouped in bins. The bin-width was dependent on the maximal displayed time and was 0.5–1 ms for the open-time and 0.1–0.2 ms for the close-time distribution. In the histograms the number of events per bin are plotted as a function of the time. In all histograms the data point corresponding to the shortest analyzed time (equal to the sampling interval) was discarded. The data points were fitted by a single- or double-exponential curve with the least-squares method. The calculated time constants were corrected for missed brief events as described by Neher [13]. For the analysis of time histograms, cell-excised (inside-out-oriented) patches containing only one single channel were used. In most experiments the patch pipette was filled with KCl solution (in mM: 140 KCl/1 $MgCl_2$/1.3 $CaCl_2$/10 Hepes, buffered to pH 7.4 with KOH) and the bath contained NaCl solution (in mM: 140 NaCl/4 KCl/1 $MgCl_2$/1.3 $CaCl_2$/10 Hepes, buffered to pH 7.4 with NaOH). In order to stimulate Cl^- channel activity, 10^{-4} M of dibutyryl cyclic AMP was added to the bath. The sign of the potential refers to the bath (cytosolic side) with respect to the patch pipette interior. Single-channel currents carried by Cl^- ions flowing from the pipette into the bath are depicted as upward currents. Data are presented as means ± S.E.

NPPB was obtained from Dr. Lang and Dr. Englert from Hoechst (F.R.G.). The structural formulae of NPPB and DPC are presented in Fig. 1. Stock solutions of NPPB were prepared by dissolving in 0.1 ml dimethylsulfoxide (DMSO) (Merck, Darmstadt, F.R.G.) and then adding 100

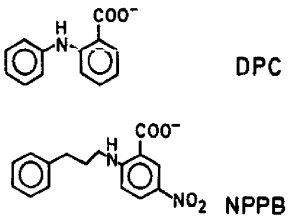

Fig. 1. Structure of DPC and NPPB.

ml of the NaCl solution. DMSO alone had no effect on the single-channel recordings.

Results

As described in a previous study [7], we observed Cl^- channels in the upward-facing cell membrane of subconfluent HT_{29} cells. The single-channel current showed outward rectification and the mean single-channel conductance was 53 ± 2 pS ($n = 13$) at positive clamp voltages. For the analysis of open- and closed-time histograms the clamp potential was in the range of +40 to +60 mV. In this voltage range we could not observe significant differences in the kinetic parameters.

Fig. 2 demonstrates the effect of 50 and 100 μM of NPPB. In the absence of the substance (control conditions), the channel is mostly in its open state, which is interrupted by brief closing events (first trace in Fig. 2). With 50 μM NPPB, the channel kinetics change markedly and many brief opening and closing events can be detected (second trace in Fig. 2). With 100 μM NPPB, only brief opening events become apparent. These opening events are so fast that they frequently do not reach their full amplitude, probably because of low-pass filtering. Therefore, kinetic analysis would be incorrect at high blocker concentrations, and we restricted the evaluation of open- and closed-time histograms to blocker concentrations of up to 50 μM.

Fig. 3 demonstrates single-channel recordings at higher time resolution under control conditions, and with 10 and 50 μM NPPB in the bath. This figure shows again that the number of closing and opening events increases with increasing blocker concentration. Fig. 4 demonstrates the corresponding open- and closed-time histograms. Under control conditions the open-time histogram could be fitted by two time constants, with 1.2 ms and 46 ms. The ratio of the areas under each exponential curve, $F1/F2$, is 0.1, and indicates that the state described by the long time constant is occupied 10-times more frequently than that represented by the short time constant. The closed-time histogram yields one time constant with 0.3 ms, which is due to the brief closing events. However, longer-lasting closing events,

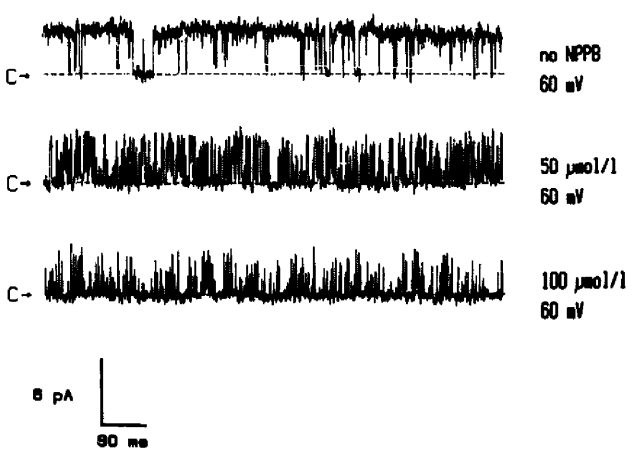

Fig. 2. Single Cl^- channel current recordings in the apical membrane of HT_{29} cells in absence of NPPB (upper trace), and with 50 μM NPPB (middle trace) and 100 μM NPPB (lower trace). C → denotes the closed state of the channel. The clamp potential was 60 mV.

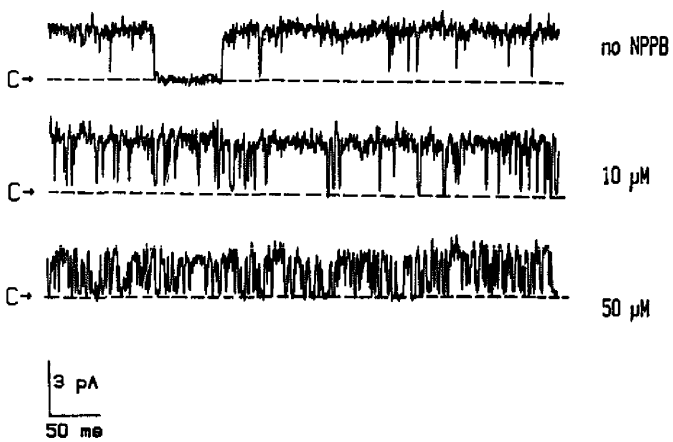

Fig. 3. Single Cl^- channel current recordings in the apical membrane of HT_{29} cells in absence of NPPB (upper trace) and with NPPB concentrations, as indicated at the right side of each trace. C → denotes the closed state of the channel. The clamp potential was 50 mV.

which are present in Fig. 3 (upper trace), would probably produce a second, longer, closed-time constant. This longer time constant is not detected in the histogram (Fig. 4) because the number of long closed events was probably too small. The open-time histogram recorded with 10 and 50 μM NPPB reveals that the long open-time constant, t_2^o, decreases with increasing blocker concentration. This behaviour reflects the interruptions of the channel open state by the blocker-induced brief closing events. The short time constant, t_1^o, vanishes at these blocker concentrations. However, some experiments with low blocker concentration (1 and 2 μM) revealed that both the short and long open-time constants were still present (data not shown). With respect to control conditions, the short time constant, t_1^o, does not change significantly, whereas the long time constant, t_2^o, decreases significantly. Therefore it is likely that, with higher NPPB concentration (at least 5 μM), the short and long time constants approach each other and can no longer be resolved in the open-time histogram. The closed-time histogram shows that with increasing blocker concentration the time constant, t_1^c, increases slightly.

Fig. 5 summarizes the dependence of the long open-time constant, t_2^o, and that of the closed-time constant, t_1^c, on the blocker concentration. The figure reveals a strong dependence of both time constants at low NPPB concentration (up to 10 μM) and a smaller change at high concentrations (30 and 50 μM). The mean open-state probability, P_o, demonstrated in Fig. 6a, reflects the effect of NPPB on the long open-time constant: P_o decreases strongly at low NPPB concentration and declines slightly at higher ones. In Fig. 6b a Hill plot of the dependence of the open-state probability on the blocker concentration is shown. On the y-axis the logarithm of $P_o/(P_{max} - P_o)$ is plotted, where $P_{max} = 0.94$ is the open-state probability under control conditions. The curve can be approximately fitted by a linear regression, yielding a Hill coefficient of 0.7. This is compatible with one NPPB molecule blocking one channel molecule.

Discussion

The present results confirm previous observations that NPPB inhibits epithelial Cl^- channels by inducing brief closing events. This causes a reduction of the mean open-state probability, whereas the single-channel conductance does not change significantly. At blocker concentrations above 50 μM the data analysis becomes difficult because of the limited time-resolution of the recording system. The current trace recorded with 100 μM NPPB, shown in Fig. 2, may mean, however, that the open-state probability is small under these conditions. The inhibitory effect of NPPB

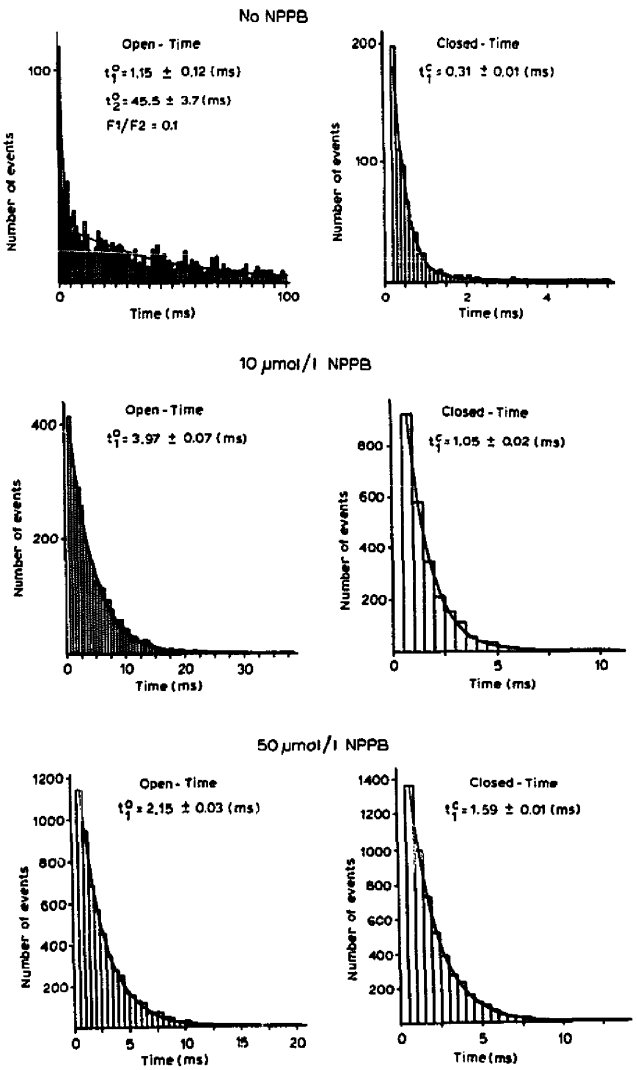

Fig. 4. Open- and closed-time histograms corresponding to the single-channel current recordings as shown in Fig. 3. The time constants, given on each histogram, were obtained from exponential fits to the data points.

on Cl^- channels in HT_{29} cells is less pronounced than its effect on the basolateral Cl^- conductance in the thick ascending limb of Henle's loop (cTALH) in the rabbit kidney [2]. This may mean that the Cl^- channels in both tissues have different characteristics. Moreover, it was reported that the dosage of NPPB required to inhibit Cl^- channels varies considerably between different tissues [4]. On the other hand, we have to consider that in the present experiments the blocker was applied to the cytosolic side, whereas it was administered to the extracellular side of the membrane in experiments with isolated perfused tubules of the cTALH.

Under control conditions the open-time histogram yields two time constants, whereas the closed-time histogram can be fitted by one exponential. This behaviour is different from previ-

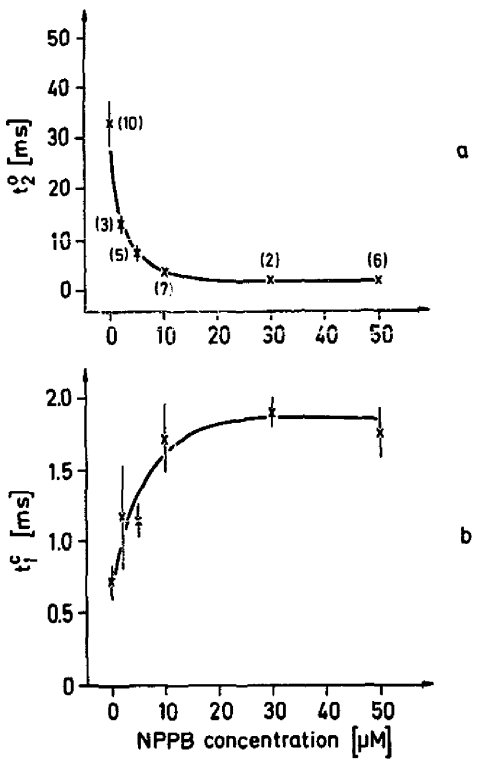

Fig. 5. Dependence of the mean long open-time constant, t_2^0 (a), and of the mean closed-time constant, t_1^c (b), on the concentration of NPPB. The numbers of experiments are given in brackets. The data points are fitted by eye.

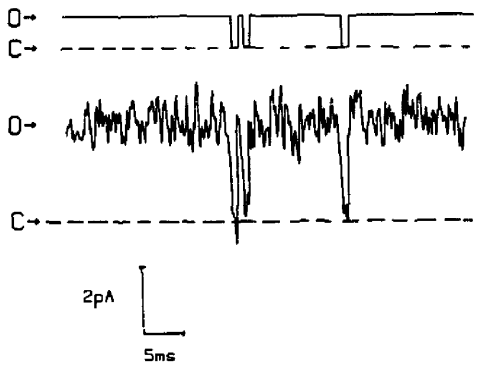

Fig. 7. Single Cl^- channel current of HT_{29} cells at high time resolution, demonstrating one short open event. On the upper part the idealized trace is depicted. C → denotes the closed state and O → the open state.

ous observations on Cl^- channels in the rectal gland of the dogfish [5] as well as in HT_{29} cells [7], where two closed-time constants were observed. This discrepancy can be explained by the fact that in the previous experiments the channel occupied its closed state more frequently, so that a second longer time constant became apparent. In the present series of experiments the channel is strongly activated, so that the longer closed-time periods are probably too infrequent to yield a second, longer, time constant.

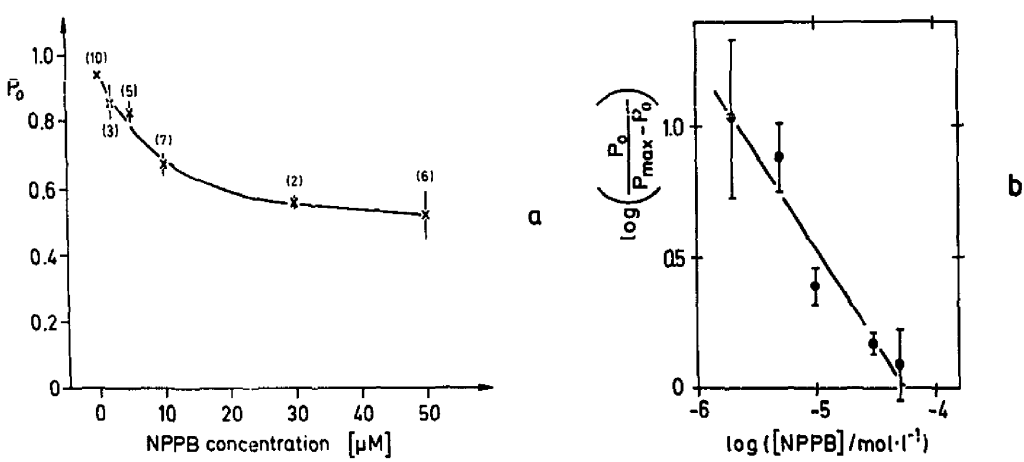

Fig. 6. (a) Dependence of the mean open-state probability, P_o, on the NPPB concentration. The numbers of experiments are given in brackets. The data points are fitted by eye. (b) Hill plot of inhibition of Cl^- channels in HT_{29} cells by NPPB. P_{max} is the open-state probability in the absence of NPPB and is equal to 0.94. The data points were fitted by linear regression, yielding a Hill coefficient of 0.7.

On a first glance, it is unexpected that the open-time distribution yields a short time constant in the range of 1 ms. Close inspection of the single-channel current traces reveals that brief opening events are interposed in the long open-time periods. One of these events is depicted in Fig. 7, together with the idealized trace. These events can be denoted as 'Nachschlag openings' in analogy to the 'Nachschlag phenomenon' detected for closing events in the nicotinic acetylcholine receptor channel [14].

The simplest kinetic scheme describing the gating characteristics of the Cl^- channel in HT_{29} cells is the following:

$$O_{long} \underset{\beta}{\overset{\alpha}{\rightleftharpoons}} C \underset{\delta}{\overset{\gamma}{\rightleftharpoons}} O_{short} \qquad \text{(Scheme I)}$$

where two open states, O_{long} and O_{short}, can be reached from one closed state, C. The rate constant are related to the time constants in the following way:

$$t_1^c = 1/\alpha \quad t_2^c = 1/\gamma$$
$$t_2^o = 1/\beta \quad t_1^o = 1/\delta$$

In this model, O_{long} represents the long open periods of the channel and O_{short} the brief 'Nachschlag openings'. The above model predicts a second closing rate constant, γ, which was, however, not detected in our experiments. This second closed-time, t_2^c, could be due to the longer closed periods, which were observed in the single-channel current recordings, but which appeared too infrequently to yield an exponential distribution in the closed-time histogram. Alternatively, it could be the case that the values of the time constants t_1^c and t_2^c are close together and cannot be resolved in the closed-time histogram. We think that the latter possibility is more likely, because both the long and the short openings were usually preceded and followed by short closures.

In the presence of the blocker, NPPB, we observed a decrease in the long open-time constant, t_2^o, and an increase in the closed-time constant, t_1^c. As pointed out above, we observed that the short open-time constant, t_1^o, is not influenced by 1 μM NPPB, but could no longer be detected at higher blocker concentrations. This is probably due to the fact that the long and short open-time constants could no longer be resolved as two superimposing exponentials. Therefore, blocker-induced alterations of the short open-time constant, t_1^o, cannot be excluded. It is remarkable that no additional time constants were detected in the presence of NPPB. The appearance of an additional time constant would be expected if the blocker were to induce a blocked state of the channel, which could be reached from one of the open states in scheme I. Such a blocked state has been observed in kinetic studies, as, for example, for the inhibition of the acetylcholine receptor channel by local anaesthetics [15] and for the block of K^+ channels by Ba^{2+} ions [16–18].

In contrast to these observations, we observed alterations of already existing time constants. Consequently, we hypothesize that binding of NPPB to a site on the channel molecule causes changes in the transitions between existing conformational states, and does not induce an additional blocked state in the kinetic diagram.

Acknowledgement

We thank Professor Dr. K.J. Ullrich for valuable discussion.

References

1 Di Stefano, A., Wittner, M., Schlatter, E., Lang, H.J., Englert, H. and Greger, R. (1985) Pflügers Arch. 405, S95–S100.
2 Wangemann, P., Wittner, M., Di Stefano, A., Englert, H.C., Lang, H.J., Schlatter, E. and Greger, R. (1986) Pflügers Arch. 407, S128–S141.
3 Greger, R., Lang, H.J., Englert, H.C. and Wangemann, P. (1987) in Diuretics II (Puschett, J.B. and Greenberg, A., eds.), pp. 131–137, Elsevier/North-Holland, Amsterdam.
4 Greger, R. (1988) Methods Enzymol., in press.
5 Greger, R., Schlatter, E. and Gögelein, H. (1987) Pflügers Arch. 409, 114–121.
6 Novak, I. and Greger, R. (1988) Pflügers Arch. 411, 546–553.
7 Hayslett, J.P., Gögelein, H., Kunzelmann, K. and Greger, R. (1987) Pflügers Arch. 410, 487–94.
8 Dreinhöfer, J., Gögelein, H. and Greger, R. (1988) Pflügers Arch. 411, R76.
9 Hamill, O.P., Marty, A., Neher, E., Sakmann, B. and Sigworth, F.J. (1981) Pflügers Arch. 391, 85–100.
10 Colquhoun, D. and Sigworth, F.J. (1983) in Single-Channel

Recording (Sakmann, B. and Neher, E., eds.), pp. 191–264, Plenum Press, New York.
11 Gögelein, H. and Greger, R. (1987) Pflügers Arch. 410, 288–295.
12 Benzanilla, F. (1985) Biophys. J. 47, 437–441.
13 Neher, E. (1983) J. Physiol. 339, 663–678.
14 Colquhoun, D., Sakmann, B. (1981) Nature 294, 464–466.
15 Neher, E. and Steinbach, J.H. (1978) J. Physiol. 277, 153–176.
16 Vergara, C. and Latorre, R. (1983) J. Gen. Physiol. 82, 543–568.
17 Miller, C., Latorre, R. and Reisin, I. (1987) J. Gen. Physiol. 90, 427–449.
18 Benham, C.D., Bolton, T.B., Lang, R.J. and Takewaki, T. (1985) Pflügers Arch. 403, 120–127.